

# Morphology and phase behaviour of blends of syndiotactic and isotactic polypropylene: 1. X-ray scattering, light microscopy, atomic force microscopy, and scanning electron microscopy

Ralf Thomann, Jörg Kressler\*, Stefan Setz, Chun Wang and Rolf Mülhaupt

Freiburger Materialforschungszentrum und Institut für Makromolekulare Chemie der Albert-Ludwigs-Universität Freiburg, Stefan-Meier-Str. 31, 79104 Freiburg i. Br., Germany  
(Received 8 August 1995; revised 6 October 1995)

Blends of isotactic and syndiotactic polypropylene were studied by wide angle X-ray scattering (WAXS), small angle X-ray scattering (SAXS), light microscopy, scanning electron microscopy and atomic force microscopy. WAXS measurements show that both polymers crystallize in different unit cells already during precipitation from a common solvent. Both polymers have a very similar long period and lamella thickness after isothermal crystallization at 135°C as revealed by SAXS. From the crystallization morphology, it can be concluded that the crystallization of isotactic and syndiotactic polypropylene after isothermal annealing in the melt occurs always in large, macroscopic domains. Isotactic polypropylene crystallizes preferably in different spherulitic forms which can usually not be detected for syndiotactic polypropylene crystallizing preferably as needle-like entities. The crystalline morphology of the blends is very complex and depends strongly on the thermal history in the melt, the crystallization temperature and blend composition. It can clearly be seen that the blends undergo liquid–liquid phase separation in the melt which yields isotactic polypropylene in a matrix of syndiotactic polypropylene; syndiotactic polypropylene in a matrix of isotactic polypropylene or a co-continuous morphology for nearly symmetric blends. Copyright © 1996 Elsevier Science Ltd.

(Keywords: syndiotactic polypropylene; isotactic polypropylene; blends; morphology)

## INTRODUCTION

In the years following the pioneering synthetic and structural work of Natta and his colleagues (e.g., ref. 1), numerous groups have aimed their research on a better understanding of the morphology of isotactic polypropylene (i-PP)<sup>2–7</sup>. There are mainly three different crystal modifications known;  $\alpha$ ,  $\beta$  and  $\gamma$ <sup>5</sup>. Five different spherulite types were identified and characterized by Norton and Keller<sup>6</sup>. For syndiotactic polypropylene (s-PP), the research was rather limited because of the lack of suitable methods to produce s-PP with a reasonably high stereoregularity in a large scale. Some recent papers deal with morphology and with thermal behaviour of melt crystallized s-PP<sup>8–14</sup>. Three different crystal modifications, types I, II and III, have been observed. Furthermore, it is known that i-PP forms a 3<sub>1</sub> helix whereas a s(2/1)2 helix is typical for s-PP. As far as we know, there does not exist a systematic investigation on the phase behaviour and morphology of i-PP/s-PP blends.

The aim of this paper is to study the morphology of i-PP/s-PP blends in the solid state and to draw

conclusions concerning their phase behaviour in the liquid state. Wide and small angle X-ray scattering (WAXS and SAXS) should provide information about the unit cells, lamella thickness and long periods of the neat polymers and the blends. Therefore, most of the samples were isothermally crystallized after isothermal annealing above the melting temperature. The morphology was then studied by polarized light microscopy, atomic force microscopy and scanning electron microscopy.

## EXPERIMENTAL

### Materials

Molecular weight data, the tacticity,  $M_w/M_n$ , and the equilibrium melting points of the polymers are given in Table 1. The molecular weights were determined by s.e.c. The tacticity was measured by <sup>13</sup>C n.m.r. and the equilibrium melting point were calculated using Hoffman–Weeks plots<sup>15</sup>. The catalyst system used for the synthesis of s-PP was Me<sub>2</sub>C(Cp)(Flu)ZrCl<sub>2</sub>/MAO (Al/Zr = 2500). The polymerization was carried out in toluene at 20°C and 2 bar propene pressure for 3 h. The catalyst concentration was 20  $\mu\text{mol l}^{-1}$  and the activity was 1460 kg PP (mol bar h<sup>-1</sup>). The catalyst used for the synthesis of

\* To whom correspondence should be addressed

**Table 1** Characteristic data of polymers used for the blends

Polymer: $M_n$ (g mol <sup>-1</sup> )	Tacticity	$T_m^0$ (°C)	$M_w/M_n$
<i>i</i> -PP	90.7% mmmm-pentads	177.2	2.3
<i>s</i> -PP	94% rrrr-pentads	155.6	2.3

*i*-PP was *rac*-Me<sub>2</sub>Si(2-Me-Benz[e]Ind)<sub>2</sub>ZrCl<sub>2</sub>/MAO (Al/Zr = 2000). The solvent decalin, obtained from Merck-Schuchardt, was dried and distilled. The methanol p.a. was obtained from Riedel-de-Haen.

#### Blend preparation

The blends were prepared by dissolving different ratios of *i*-PP and *s*-PP in hot decalin (1 wt% total). The solution was precipitated into a 20 fold excess of methanol. The blends were then washed with methanol and dried in a vacuum oven at 60°C for 2 days.

#### X-ray measurements

The precipitated samples were dried and the powder was directly used for WAXS measurements using the standard procedure. The measurements were carried out with a Siemens D500 apparatus. For WAXS and SAXS measurements a CuK $\alpha$  radiation of a wavelength  $\lambda = 0.154$  nm was used. The samples for SAXS measurements were isothermally crystallized at 135°C. An evacuated Kratky compact camera (Anton Paar K.G.) with an entrance slit of 80  $\mu$ m was used. The scattering profiles were corrected for background scattering and desmeared<sup>16</sup>. The contribution of thermal density fluctuations to the scattering intensity are eliminated by computing the slope of an  $Iq^4$  versus  $q^4$  plot at high scattering vectors,  $q = (4\pi/\lambda)\sin(\theta/2)$  where  $I$  is the scattering intensity and  $\theta$  is the scattering angle. The Fourier transformation of the scattering curve yields the linear correlation function  $K(z)$  defined by<sup>17,18</sup>

$$K(z) = \int_0^\infty 4\pi q^2 I(q) \cos^2 \pi q z dq \quad (1)$$

#### Light microscopy

The samples used to study the phase behaviour by light microscopy were prepared by melting the powder of the neat polymers or the blends between two cover glasses. The layer thickness between the glasses was about 40  $\mu$ m. The samples were held for 10 min at 180°C and then quenched to crystallization temperature with a rate of 30°C min<sup>-1</sup>. The light microscopy investigations were carried out with an Olympus-Vanox AH2 microscope and a Linkam TMS 90 hot stage that allows observation during isothermal crystallization.

The two-layer specimens for diffusion experiments were made by crystallizing samples of *s*-PP and *i*-PP between cover glasses. The as-received thin films were removed from the cover glasses by putting them into water for several days. After drying, films with a plane surface were received. These films of *s*-PP and *i*-PP were slightly pressed together. Between two cover glasses they were molten together, and held at 180°C for 5 h. Then, they were crystallized together at 126°C, the cover glasses were again removed in water, and the film was cut in an ultramicrotome (Reichert & Jung) with a layer thickness of about 2  $\mu$ m.

The sample for the nucleation experiment was made by melting powder of *i*-PP and *s*-PP together between two cover glasses, in a way, that the *s*-PP and the *i*-PP were separated, until the melts flow together. The sample was crystallized at 130°C. The contact zone between the two phases was examined between crossed polarizers.

The samples used to study the melt morphology were isothermally annealed for about 5 days at various temperatures, and then quenched in liquid nitrogen. This was carried out in a way that the phase with mainly *i*-PP crystallizes and the phase with mainly *s*-PP does not.

#### Atomic force microscopy

The etching reagent was prepared by stirring 0.02 g potassium permanganate in a mixture of 4 ml sulfuric acid (95–97%) and 10 g orthophosphoric acid. The 80  $\mu$ m thick films of the blends were immersed into the fresh etching reagent at room temperature and held there for 14 h. In the beginning, the sample was held in an ultrasonic bath for 30 min. For subsequent washings, a mixture of 2 parts by volume of concentrated sulfuric acid and 7 parts of water was prepared and cooled to near the freezing point with dry ice in iso-propanol. The samples were washed successively with 30% aqueous hydrogen peroxide (to remove any manganese dioxide or permanganate present). Then the samples were washed with distilled water and methanol. Each washing was supported with an ultrasonic bath. The AFM experiments were carried out with a 'Nanoscope III' scanning probe microscope (Digital Instruments, Inc.) at ambient conditions. The measurements were performed in the height mode. Si tips (Nanoprobes) were employed with a force constant of about 0.1 N m<sup>-1</sup>.

#### Scanning electron microscopy

The specimens were made by pressing the *i*-PP/*s*-PP blends at 180°C for 10 min. The sample showing the co-continuous morphology was then isothermally annealed for 10 min at 135°C, quenched rapidly in ice water, cut with a razor blade, dipped into toluene for 10 min at a temperature of 70°C, washed with cold toluene and acetone and dried in vacuum for 48 h. The sample for cryofracture was annealed for 16 h at 135°C for space filling crystallization and quenched in ice water. The specimen was stored in liquid nitrogen for 10 min and then rapidly broken just above the surface of the liquid. Both samples were sputtered with gold in a Scientific-Instruments mini coater (air 200 mbar, 20 mA, 2 min). A scanning electron microscope (Zeiss DSM 960) was used in secondary electron mode.

## RESULTS AND DISCUSSION

#### X-ray measurements

The upper three curves of Figure 1 show the WAXS measurements of neat *i*-PP, neat *s*-PP and a 50/50 (wt%) blend. All samples were prepared by precipitating a 1 wt% decalin solution of the respective polymers in methanol and then dried. It can be seen that neat *i*-PP crystallizes in the  $\alpha$ -modification. The peak at  $q = 13.3$  nm<sup>-1</sup> can be assigned exclusively to the  $\alpha$ -phase<sup>19</sup>. The characteristic peak of the  $\gamma$ -modification at a scattering vector of  $q = 14.3$  nm<sup>-1</sup> cannot be found<sup>20</sup>. The second curve from the top belongs to neat *s*-PP. Most of the sample forms the lattice type II<sup>21</sup>. The

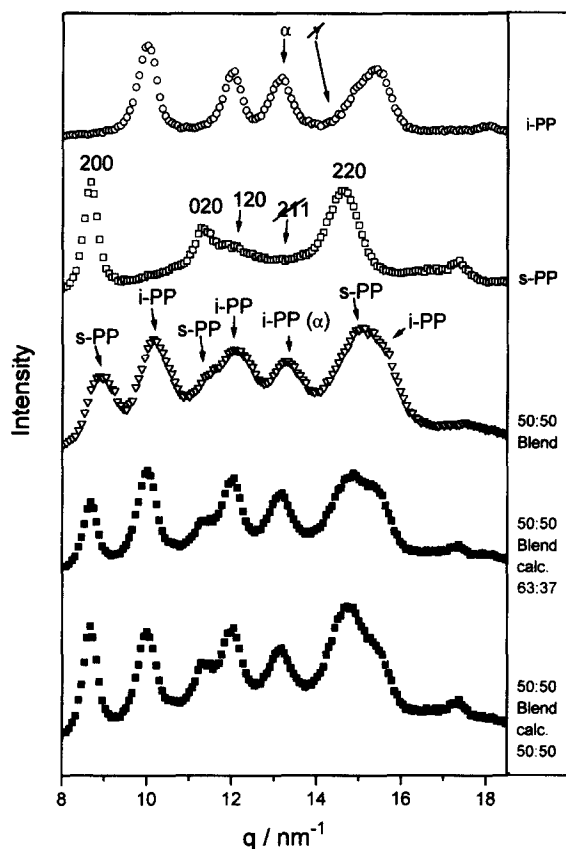


**Figure 1** WAXS powder diffraction spectra of *i*-PP, *s*-PP and a 50/50 (wt%) blend precipitated from a common solvent. The two bottom traces for the blend are calculated (see text)

characteristic reflex for the lattice type III cannot be detected. The third curve from the top shows that the experimentally obtained blend pattern is simply composed of *i*-PP and *s*-PP contributions. The two curves at the bottom are calculated assuming additivity of the pattern of the neat components with a different weight. As can be seen, the best fit is obtained assuming an *i*-PP/*s*-PP ratio of 63/37 wt% in the crystalline phase. This is caused by the fact that during the precipitation *i*-PP crystallizes faster than *s*-PP, which is in agreement with a faster rate of crystallization of *i*-PP from the melt at large supercoolings compared to *s*-PP<sup>22</sup>.

*Figure 2* shows the correlation function for neat *i*-PP, *s*-PP and a 50/50 (wt%) blend isothermally crystallized at 135°C. It can be seen that both polymers have a similar lamella thickness represented by the first minimum and a long period represented by the first maximum of the correlation function. The lamella thickness for *i*-PP is about 9 nm, the long period is about 20 nm. The corresponding values for *s*-PP are 10 and 20 nm. Because of the small difference of these values, it is impossible to judge from SAXS measurements of the blends if one or two types of lamellae with a different thickness are present. Thus the correlation function of the blend appears like that one of a single species. It should be mentioned that the *s*-PP seems to be more ordered compared to the *i*-PP sample because the second minimum and maximum in the correlation function are more pronounced for neat *s*-PP. From WAXS measurements, it can be concluded that *i*-PP and *s*-PP crystallize separately even during the very fast precipitation process

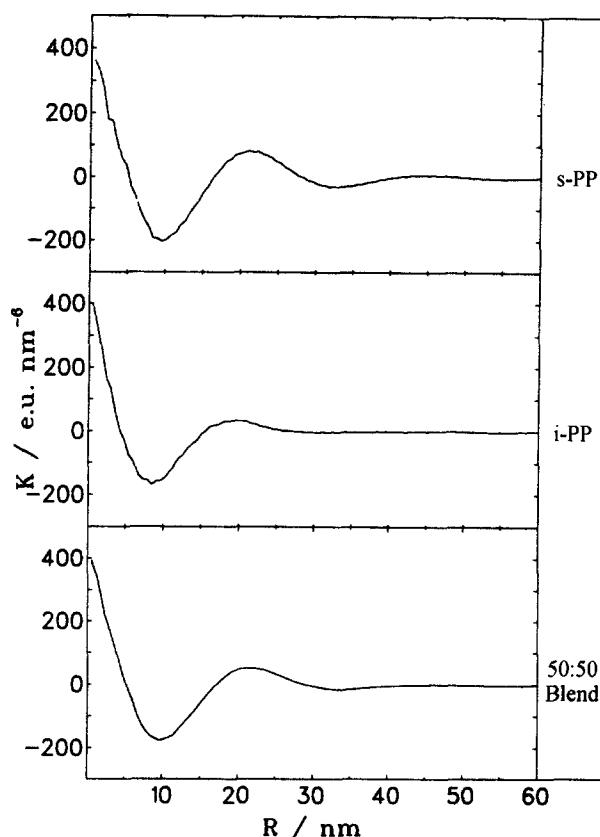
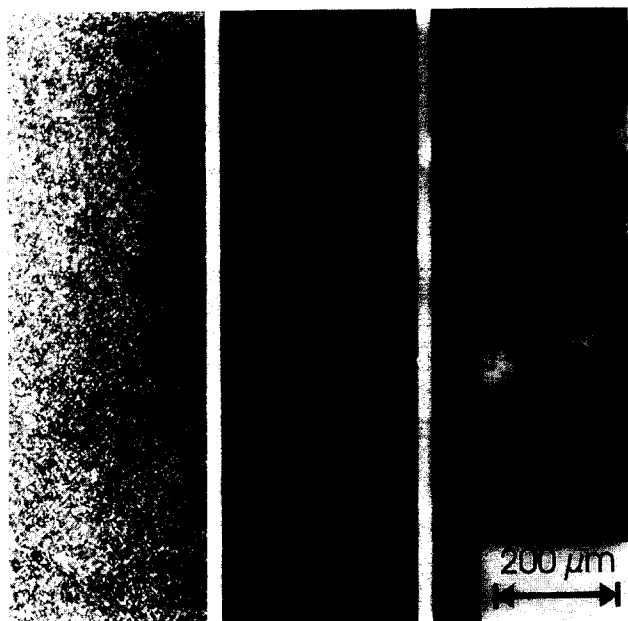


**Figure 2** Correlation function obtained from SAXS measurements for *i*-PP, *s*-PP and a 50/50 (wt%) blend isothermally crystallized at 135°C

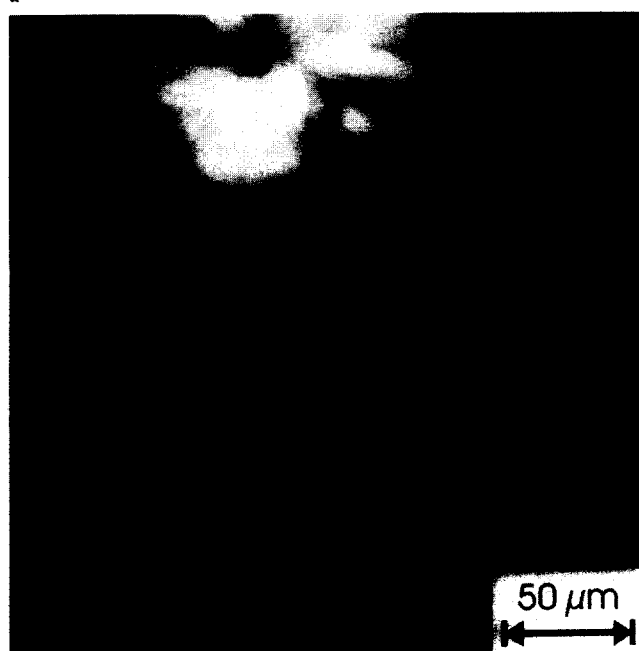
from a common solvent. SAXS measurements are inconclusive with respect to the miscibility because both polymers have a very similar lamella thickness and long period after isothermal crystallization at 135°C.

#### Phase behaviour

In order to judge the miscibility of *s*-PP and *i*-PP, microscopic techniques are employed. Above the melting point all blends, independent of the blend ratio and annealing temperature, are transparent. The samples for light microscopy are annealed for different time intervals at 180°C, just above the equilibrium melting point of the polymers, and immediately quenched in liquid nitrogen. Quenching of phase morphologies from the melt to the solid state is a frequently used method in order to study the phase behaviour of polymer blends<sup>23–28</sup>. The morphology of a 50/50 (wt%) blend molten at 180°C, immediately quenched in liquid nitrogen, and observed by polarized light microscopy can be seen in the left side of *Figure 3a*. The whole sample shows a crystalline, mosaic-like structure. No indication of liquid–liquid phase separation prior to crystallization is found. The situation changes dramatically after annealing the blend for 5 days at 180°C as can be seen in the middle part of *Figure 3a*. A kind of co-continuous phase morphology can be observed. This should be the result of a liquid–liquid phase separation prior to the crystallization process. The contrast in the polarized light micrograph arises from the fact that upon quenching the *i*-PP crystallizes faster than the *s*-PP thus forming the bright phase<sup>22</sup>. This can even better be distinguished in the right side of *Figure 3a* and in *Figure 3b*. Here the sample was



a



b

**Figure 3** Polarized light micrographs of 50/50 (wt%) blends of *i*-PP and *s*-PP. The samples were prepared by precipitation from a common solvent and then thermally annealed. (a): (Left)—molten at 180°C and then immediately quenched in liquid nitrogen; (middle)—annealed for 5 days at 180°C and quenched in liquid nitrogen; (right)—molten at 180°C, annealed for 5 days at 150°C, and quenched in liquid nitrogen. (b) As *Figure 3a* (right) but different magnification

annealed for 5 days at 150°C. At this temperature the same liquid–liquid phase separation takes place but the annealing temperature is below the equilibrium melting points of both polymers. The supercooling is larger for *i*-PP and therefore *i*-PP is able to crystallize very slowly even before the quenching. As a result, well-formed spherulites of *i*-PP can be observed. Their growth is mainly confined by the phase boundary previously formed by liquid–liquid phase separation. Especially in *Figure 3b*, it can be seen that their growth stops at the boundary of the *i*-PP rich phase. The lower spherulite shows some fibrils growing into the *s*-PP rich phase. Thus



**Figure 4** SEM micrograph of a co-continuous phase morphology of a 50/50 (wt%) blend of *i*-PP and *s*-PP annealed for 10 min at 180°C, then crystallized for 10 min at 135°C and finally quenched in ice water and etching in toluene at 70°C. Toluene removes the *s*-PP phase selectively

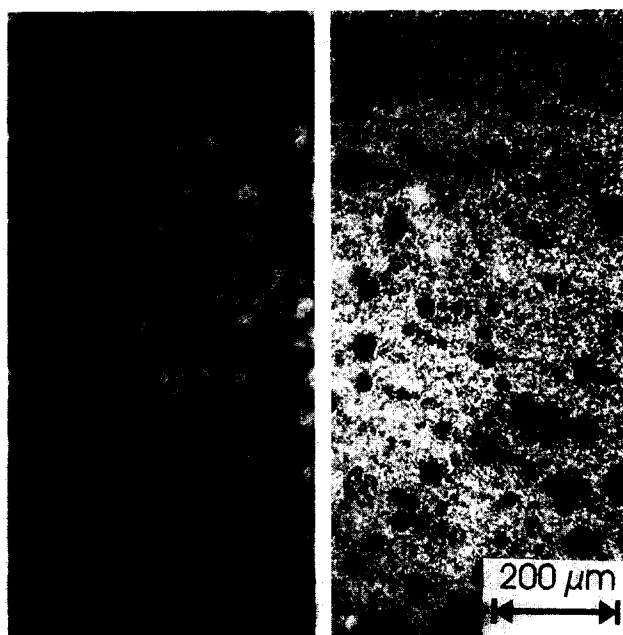


**Figure 5** Polarized light micrographs of *i*-PP/*s*-PP blends annealed for 5 days at 180°C and quenched in liquid nitrogen. (Left) *i*-PP/*s*-PP 20/80 (wt%), (right) *i*-PP/*s*-PP 80/20 (wt%)

it can be seen that mixed phases are formed where always one of the both polymers is enriched. *Figure 4* shows an SEM micrograph of an *i*-PP/*s*-PP 50/50 (wt%) sample isothermally pressed at 180°C for 10 min, then kept for 10 min at 135°C and finally quenched in ice water. The *s*-PP phase was removed in toluene at 70°C. A co-continuous morphology can be observed. This kind of phase morphology can frequently be observed after liquid–liquid phase separation in polymer blends via spinodal decomposition<sup>29</sup>.

The morphology changes also very much with varying blend compositions. *Figure 5* (left side) shows a polarized light micrograph of an *i*-PP/*s*-PP 20/80 (wt%) blend annealed for 5 days at 180°C and then quenched in liquid nitrogen. It can be seen that the *s*-PP rich phase (dark) forms the matrix. *i*-PP is able to crystallize faster and forms thus a dispersed phase (bright). The opposite can

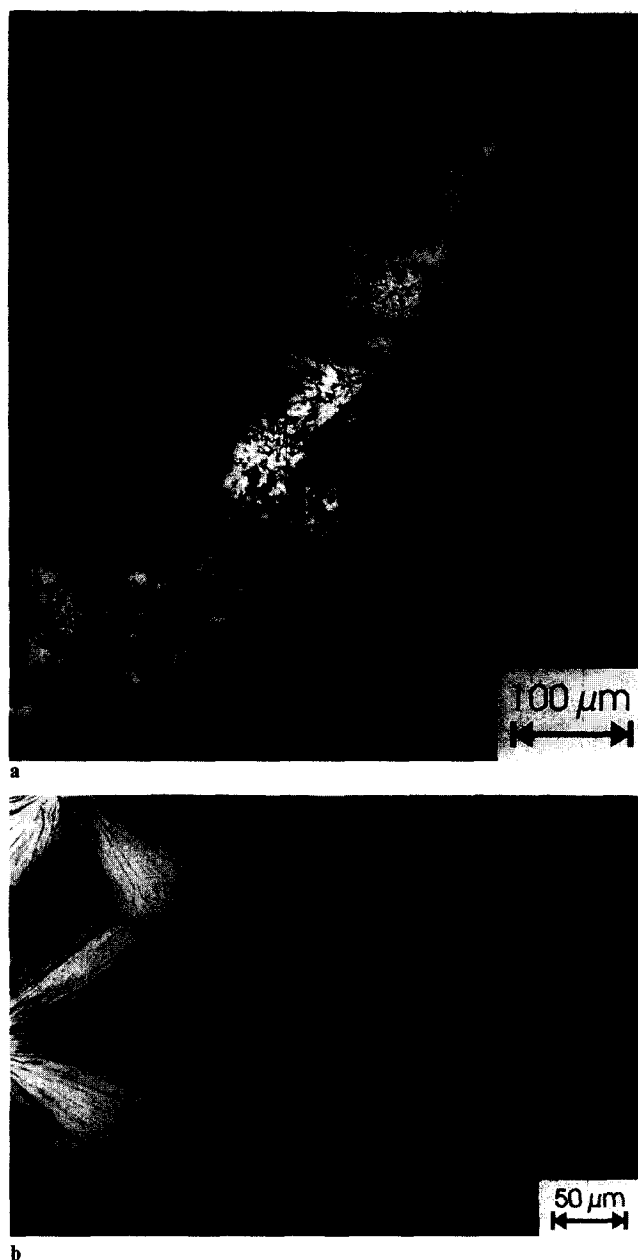


**Figure 6** (a) Polarized light micrograph of a two-layer specimen of *s*-PP (bottom) and *i*-PP (top) annealed for 5 h at 180°C. (b) Nucleation at the interface between *s*-PP and *i*-PP isothermally crystallized at 130°C

be observed for an *i*-PP/*s*-PP 80/20 (wt%) sample with the same thermal history. Here, the continuous phase is formed by the *i*-PP rich phase (bright) and the *s*-PP is dispersed (dark).

It is often useful to study the mixing process instead of the demixing process in order to judge polymer miscibility. A frequently used method is to study diffusion processes in two-layer specimens<sup>30</sup>. Therefore, two-layer specimens of *i*-PP and *s*-PP are prepared in order to verify the results obtained by studying polymer blends. Figure 6a shows a two-layer specimen of *i*-PP and *s*-PP annealed for 5 h at 180°C and then isothermally crystallized at 126°C. It was crystallized between glass plates because this prevents the formation of transcrystals which are formed by other substrates acting as nucleation agents<sup>31</sup>. In the case of miscibility an interdiffusion process should be observed. But in the

case of an *i*-PP (top layer)/*s*-PP (bottom layer) sample, it can clearly be seen that a sharp interface without any interdiffusion is formed. This supports the previous experimental findings that *i*-PP and *s*-PP are immiscible. Figure 6b shows the interfacial area of a sample where *i*-PP and *s*-PP were molten separately at 180°C. The melts are then slowly brought into contact and rapidly cooled to the crystallization temperature of 130°C. It can be seen that *s*-PP (right) acts as a nucleation agent for *i*-PP (left) which forms large spherulites. As in the two-layer specimens, the nucleus of *i*-PP spherulites is exactly located at the interface. The nucleation efficiency is not too high otherwise perfect transcrystals would be formed.

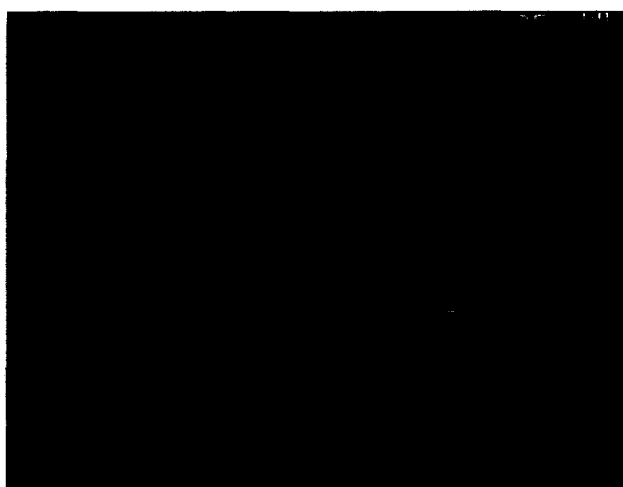
A very careful inspection of the interfacial area between *i*-PP and *s*-PP shows that the polymers can penetrate slightly during the crystallization process (but not in the melt). Figure 7a shows an AFM micrograph of the interfacial area between *i*-PP and *s*-PP of a sample isothermally crystallized at 135°C. At the right-hand side the typical appearance of *i*-PP spherulites with straight growing fibrils can be observed. The left-hand side shows the typical structures of *s*-PP which are discussed in detail elsewhere<sup>11</sup>. The occurrence of an apparently ordered and elongated structure in the interface is identical with the phenomenon discussed in Figure 3b. Because both phases are mixed phases, *i*-PP fibrils of the spherulites are able to grow to a certain extent into the *s*-PP rich phase. This can more clearly be seen in the SEM micrograph of Figure 7b. The interface has a cog-wheel like appearance caused by the interpenetration of fibrils.

#### Crystallization behaviour

There are three effects which have a forming influence on the crystalline morphology of the blends; separate crystallization of *s*-PP and *i*-PP, liquid-liquid phase separation in the melt, and different crystallization rates as a function of crystallization temperature. The spherulites of *i*-PP formed during the isothermal crystallization at 135°C are well-known<sup>6</sup>. The *s*-PP sample appears after space filling crystallization at 135°C completely different. A mosaic-like structure is formed and discussed in detail elsewhere<sup>11</sup>. The morphologies of the neat polymers can be seen in Figure 6b. The 50/50 (wt%) blend crystallized at 135°C seems to be very much influenced by the *s*-PP crystallization because large spherulites cannot be observed (Figure 8). The development of this morphology can be explained by studying the early stages of the growth of both neat polymers. Figure 9 (left side) represents an example for the crystallization of the 50/50 (wt%) blend isothermally crystallized for 3 h and 40 min at 135°C. The light micrograph obtained with not completely crossed polarizers shows that spherulites start to grow. These spherulites can also be observed between crossed polarizers. But it is typical that for this crystallization temperature also needle-like entities start to grow between the spherulites which belong to neat *s*-PP. Thus it can be concluded that at 135°C both polymers have a comparable crystal growth rate. In the regions with needle-like entities, the growth of spherulites is impossible, thus leading to large areas with a dominating *s*-PP structure. Also because the spherulites are very disordered, the otherwise typical impingement lines after space filling crystallization cannot be observed. The



a



b

**Figure 7** (a) AFM micrograph of the phase boundary between *i*-PP and *s*-PP in a 50/50 (wt%) blend isothermally crystallized at 135°C. (b) SEM micrograph of the *i*-PP/*s*-PP phase boundary of the same sample

situation changes after isothermal crystallization of the same blend at 120°C. *Figure 9* (right side) shows the same blend after a crystallization time of 1 min and 15 s at 120°C. There is a large number of spherulites but the typical needle-like entities of the *s*-PP crystallization cannot be observed. This is caused by the fact that the crystallization rate of *s*-PP at this temperature is much lower compared to *i*-PP which will be discussed in detail in the second part of this contribution<sup>22</sup>. The crystallization rates for both polymers decrease with increasing temperature in the range from 100 to 140°C, but the crystallization rate of *s*-PP decreases more slowly because it is a weaker function of temperature. Thus the *s*-PP crystallizes at high crystallization temperatures relatively faster than *i*-PP. But at the relatively low crystallization temperature of 120°C, *i*-PP crystallizes faster than *s*-PP. The growing spherulites in the blends lose their characteristic shape completely after space filling crystallization occurred. But the crystallization is not finished. The structures become brighter between crossed polarizers even after space filling crystallization occurred. This can be related to the *s*-PP contribution, whose crystallization increases the birefringence.

Also the needle-like entities of *s*-PP were studied in more detail by AFM. As already reported<sup>11</sup>, the needle-

like entities of *s*-PP are related to two different *s*-PP morphologies. There are single-crystal like entities as shown in *Figure 10* and the second morphology is formed by bundle-like structures<sup>11</sup>. All these structures are also found in the blend. *Figure 10* is very interesting because here a rotational twinning of the single crystal like entities can be observed. The twinning, i.e. the growth of daughter lamellae, occurs under an angle of 50° as predicted by Lovinger *et al.*<sup>9</sup>. The holes at the surface are formed by a certain kind of cracks which are discussed in detail in the literature<sup>9</sup>.

As already discussed for symmetric blends [*Figures 3a* (right side) and *b*], the appearance of spherulites is influenced by the liquid-liquid phase separation. An open spherulite of *i*-PP in an *i*-PP/*s*-PP 20/80 (wt%) blend can be seen in *Figure 11a*. The sample was molten at 180°C for 5 min, then quenched to the crystallization temperature of 150°C, isothermally crystallized for 5 days and quenched in liquid nitrogen. The open spherulite can be observed after the crystallization at 150°C, whereas the phase morphology is revealed only after quenching the sample in liquid nitrogen. Because of the very low crystallization rates of *i*-PP and *s*-PP at 150°C, the sample is able to undergo liquid-liquid phase separation even below the equilibrium melting point. For this blend ratio, the matrix is the *s*-PP rich phase. But the



**Figure 8** Morphology of 50/50 (wt%) blend, isothermally annealed at 180°C for 5 min and then rapidly quenched to the crystallization temperature of 135°C

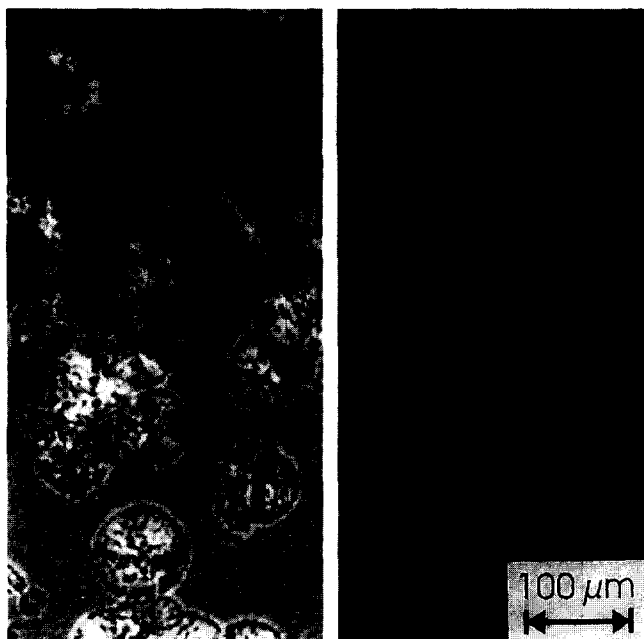


**Figure 9** Light micrographs obtained between not completely closed polarizers of an *i*-PP/*s*-PP blend 50/50 (wt%) isothermally annealed at 180°C for 5 min and then isothermally crystallized. (Left) at 135°C for 3 h 40 min, (right) at 120°C for 1 min 15 s

*i*-PP spherulite is able to grow across the matrix because it contains also a certain amount of *i*-PP. Caused by the limited amount of *i*-PP in the matrix, the spherulite can not grow uniformly but remains open. It was proved by measuring the melting point of this spherulite that it is composed of *i*-PP. A different type of spherulite was found for an *i*-PP/*s*-PP 80/20 (wt%) blend having an identical thermal history. Here the matrix is mainly composed of *i*-PP and thus the *i*-PP spherulite contains inclusions of *s*-PP which are completely surrounded by *i*-PP fibrils (*Figure 11b*).

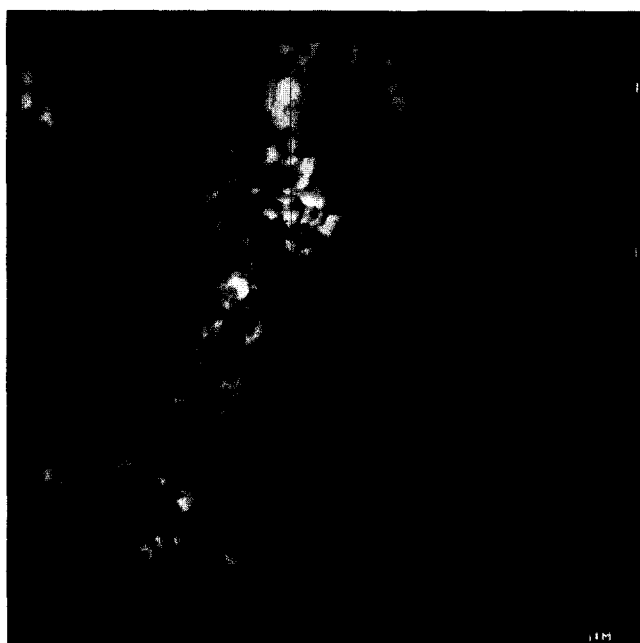


**Figure 10** Single-crystal like entity of *s*-PP after isothermal crystallization at 139°C, showing rotational twinning

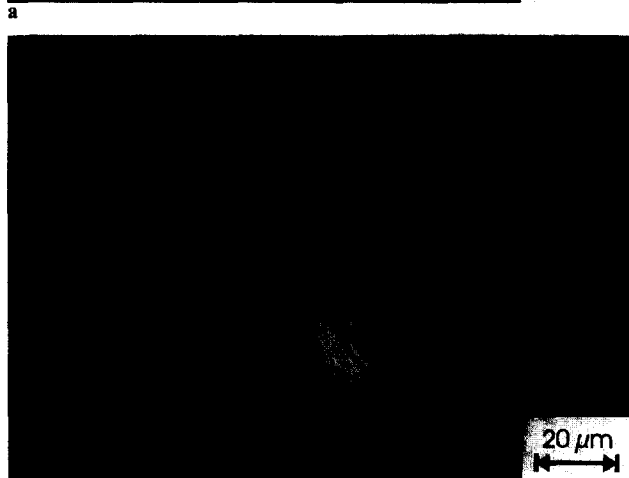


**Figure 11** Polarized light micrographs of *i*-PP/*s*-PP blends annealed for 5 min at 180°C, isothermally crystallized at 150°C for 5 days and then quenched in liquid nitrogen. (a) Open *i*-PP spherulite of a 20/80 (wt%) blend (the matrix is *s*-PP), (b) *i*-PP spherulites of 80/20 (wt%) blends grown in an *i*-PP matrix

## CONCLUSION

Apparent single phase mixtures of *s*-PP and *i*-PP are formed by precipitation from a common solvent because phase separation cannot be observed by light microscopy of samples kept above the melting point. But WAXS measurements showed already that the crystallization of *i*-PP and *s*-PP precipitated from a common solvent occurred always separately. During thermal annealing above or even slightly below the equilibrium melting points of the polymers, the blends phase separate in a spinodal decomposition like mechanism which can be observed only after the samples are partially crystallized. This yields a co-continuous phase morphology for nearly symmetric polymer blends. The crystalline morphology is widely determined by the crystallization behaviour of the neat components. Only in the interfacial area of *i*-PP and *s*-PP enriched phases, a cog-wheel like morphology is formed by interpenetrating fibrils.

## ACKNOWLEDGEMENTS

The authors would like to thank the Bundesminister für Wirtschaft for supporting this research as part of the AiF-Project 8529. We also gratefully acknowledge synthetic support by Dr S. Jüngling who supplied us with isotactic and syndiotactic polypropylene samples.

REFERENCES

- 1 Natta, G., Pasquon, I., Corradini, P., Peraldo, M., Pegoraro, M. and Zambelli, A. *Rend. Acc. Naz. Lincei* 1960, **28**, 539
- 2 Khoury, H. *J. Res. Natl. Bur. Std.* 1966, **70A**, 29
- 3 Padden, F. J. and Keith, H. D. *J. Appl. Phys.* 1966, **37**, 4013
- 4 Padden, F. J. and Keith, H. D. *J. Appl. Phys.* 1973, **44**, 1217
- 5 Basset, D. C. and Olley, R. H. *Polymer* 1984, **25**, 935
- 6 Norton, D. R. and Keller, A. *Polymer* 1985, **26**, 704
- 7 Lotz, B., Wittmann, J. C., Stocker, W., Magonov, S. N. and Cantow, H. J. *Polym. Bull.* 1991, **26**, 209
- 8 Lovinger, A. J., Davis, D. D. and Lotz, B. *Macromolecules* 1991, **24**, 552
- 9 Lovinger, A. J., Lotz, B., Davis, D. D. and Schumacher, M. *Macromolecules* 1994, **27**, 6603
- 10 Schumacher, M., Lovinger, A. J., Agarwal, P., Wittmann, J. C. and Lotz, B. *Macromolecules* 1994, **27**, 6956
- 11 Thomann, R., Wang, Ch., Kressler, J., Jüngling, S. and Mülhaupt, R. *Polymer* 1995, **36**, 3795
- 12 Balbontin, G., Dainelli, D. and Galimberti, M. *Makromol. Chem.* 1992, **193**, 693
- 13 Sozzani, P., Simonutti, R. and Galimberti, M. *Macromolecules* 1993, **26**, 5782
- 14 Stocker, W., Schumacher, M., Graff, S., Lang, J. J., Wittmann, J. C., Lovinger, A. J. and Lotz, B. *Macromolecules* 1994, **27**, 6948
- 15 Hoffmann, J. D. and Weeks, J. J. *J. Res. Natl. Bur. Stand., Sect. A* 1962, **66A**, 13
- 16 Strobl, G. R. *Acta Crystallogr.* 1970, **A26**, 367
- 17 Strobl, G. R., Schneider, M. J. and Voigt-Martin, I. G. *J. Polym. Sci., Polym. Phys. Ed.* 1980, **18**, 1361
- 18 Tanabe, Y., Strobl, G. R. and Fischer, E. W. *Polymer* 1986, **27**, 1147
- 19 Turner-Jones, A. *Polymer* 1971, **12**, 487
- 20 Rieger, B., Mu, X., Mallin, D. T., Rausch, M. D. and Chien, J. C. W. *Macromolecules* 1990, **23**, 3559
- 21 De Rossa, C. and Corradini, P. *Macromolecules* 1993, **26**, 5715
- 22 Thomann, R., Kressler, J., Rudolf, B. and Mülhaupt, R. *Polymer* 1996, **37**, 2635
- 23 Inaba, N., Yamada, T., Suzuki, S. and Hashimoto, T. *Macromolecules* 1988, **21**, 407
- 24 Hill, M. J. and Barham, P. J. *Polymer* 1992, **33**, 4891
- 25 Puig, C. C., Hill, M. J. and Barham, P. J. *Polymer* 1992, **34**, 3117
- 26 Hill, M. J. and Barham, P. J. *Polymer* 1995, **36**, 1523
- 27 Puig, C. C., Odell, J. A., Hill, M. J., Barham, P. J. and Folkes, M. J. *Polymer* 1994, **35**, 2452
- 28 Hill, M. J., Barham, P. J. and v. Ruiten, J. *Polymer* 1993, **34**, 2975
- 29 Hashimoto, T. in 'Material Science and Technology' (Eds R. W. Hahn, P. Haasen and E. J. Kramer), VCH, Weinheim, 1993
- 30 Hobbs, S. Y., Watkins, V. P. and Bendler, J. T. *Polymer* 1990, **31**, 1663
- 31 Setz, S., Schnell, R., Thomann, R., Kressler, J. and Mülhaupt, R. *Macromol. Rapid Commun.* 1995, **16**, 81